Journal of Biomolecular NMR, **11:** 185–190, 1998.
KLUWER/ESCOM

High-resolution detection of five frequencies in a single 3D spectrum: HNHCACO – a bidirectional coherence transfer experiment

Yuxi Pang[a], Lei Zeng[a,*], Alexander V. Kurochkin[a] & Erik R.P. Zuiderweg[a,b,c,**]
[a]*Biophysics Research Division,* [b]*Department of Biological Chemistry, and* [c]*Department of Chemistry, University of Michigan, 930 N. University Avenue, Ann Arbor, MI 48109-1055, U.S.A.*

Received 28 August 1997; Accepted 6 October 1997

Key words: bidirectional coherence transfer, Binase, gradient coherence selection, HNHCACO, simultaneous ^{15}N and $^{13}C^{\alpha}$ acquisition

Abstract

A new triple-resonance pulse sequence, 3D HNHCACO, is introduced and discussed, which identifies sequential correlations of the backbone nuclei (H^{α}(i–1), C^{α}(i–1), C'(i–1), NH(i), N(i)) of doubly labeled proteins in H_2O. The three-dimensional (3D) method utilizes a recording of ^{15}N and ^{13}C resonances in a single indirect time domain, the $^{13}C'$ resonance in another indirect time domain, and detects both NH and H^{α} protons. A bidirectional coherence transfer (NH(i) $\leftrightarrow$ N(i) $\leftrightarrow$ C'(i–1) $\leftrightarrow$ C^{α}(i–1) $\leftrightarrow$ H^{α}(i–1)) is effectuated, resulting in a single high-resolution 3D spectrum that contains the frequencies of all five backbone nuclei. The experiment was applied to the 12.3 kDa ribonuclease from *Bacillus intermedius* (Binase).

Multidimensional, multinuclear NMR spectroscopy is important for the determination of larger protein structures in solution (Fesik and Zuiderweg, 1988; Ikura et al., 1990a,b; Kay et al., 1990; Montelione and Wagner, 1990; Clore and Gronenborn, 1993). For $^{15}N/^{13}C$-labeled proteins, triple-resonance methods such as HNCO, HNCA, HN(CO)CA, HCACO and HA(CACO)NNH are generally used to obtain sequence-specific assignments of the backbone resonances (Montelione and Wagner, 1990; Bax and Ikura, 1991; Boucher et al., 1992; Clubb and Wagner, 1992; Grzesiek and Bax, 1992; Szyperski et al., 1993; Jahnke and Kessler, 1994). In these experiments, each backbone nucleus resonance is labeled along a separate frequency dimension, and assignment generally proceeds from the analysis of either many complementary spectra of low dimensionality or from a few self-contained spectra of high dimensionality.

Here we present a new pulse scheme, referred to as 3D HNHCACO in which five frequencies are sampled in only three dimensions. As such, the experiment combines the advantage of low dimensionality, i.e., high digital resolution, with the advantage of measuring many frequencies in a single spectrum, i.e., convenient and reliable analysis. The experiment records all five frequencies in the pathways $^{1}H^{\alpha}(i) \rightarrow {}^{13}C^{\alpha}(i) \rightarrow {}^{13}CO(i) \rightarrow {}^{15}N(i+1) \rightarrow {}^{1}HN(i+1)$ and vice-versa, and thus delineates the so-called pseudo-amino acid residues (Brutscher et al., 1995). The essential innovations in the experiment are the simultaneous recording of 3D HNCO and 3D HACACO experiments combined with a bidirectional transfer period. This method has a sensitivity comparable with HACA(CO)NNH (Boucher et al., 1992) which also records the frequencies of four or five of the nuclei in the same pathway, but which utilizes four or five dimensions to accomplish this.

Simultaneous acquisition of $[^{15}N,^{1}H]$ and $[^{13}C,^{1}H]$-correlation in heteronuclear experiments has been introduced in recent years by several groups (Sørensen, 1990; Farmer and Müller, 1991; Boelens et al., 1994; Mariani et al., 1994; Sattler et al., 1995). The experiments always contain transfer periods in which the simultaneous labeling of ^{15}N and ^{13}C coherences occurs. The different spectral widths can be accommo-

*Present address: The Mount Sinai School of Medicine, New York, NY 10029, U.S.A.
**To whom correspondence should be addressed.

dated by adjusting the sampling rates. The concept of simultaneous experiments has been applied primarily in time-consuming experiments, such as 4D HSQC-NOESY-HSQC (Ikura et al., 1990a,b; Clore et al., 1991; Zuiderweg et al., 1991). Kay and co-workers published a CN NOESY-HSQC experiment, which allowed the simultaneous recording of ^{15}N- and ^{13}C-edited NOE spectra (Pascal et al., 1994); Farmer and Müller (1994) applied this approach to a gradient-enhanced and sensitivity-enhanced 4D NOESY experiment to permit the simultaneous acquisition of a [^{13}C,^{15}N]/[^{15}N,^{15}N]-separated data set.

Figure 1 illustrates the pulse sequence for performing the 3D HNHCACO experiment. The sequence begins with a simultaneous INEPT from $^{1}H^{\alpha}$ to $^{13}C^{\alpha}$ and NH to ^{15}N in the time period a–b. ^{15}N and ^{13}C refocussing pulses are given asymmetrically to optimize for both NH $\rightarrow$ ^{15}N and $^{1}H^{\alpha} \rightarrow {}^{13}C^{\alpha}$ magnetization transfer. The 90° pulse on ^{13}C (point c) completes the ^{13}C transfer, while 2NzHz longitudinal two-spin order is maintained. Between c and d, the $^{13}C^{\alpha}$ coherence evolves under the influence of $^{13}C^{\alpha}$ chemical shifts and is labeled. After a time 2Tc (point d), the $^{13}C^{\alpha}$ magnetization becomes antiphase with respect to $^{13}C'$, and is stored as 2CzC′z following the 90° $^{13}C^{\alpha}$ pulse. The ^{15}N transfer is subsequently effectuated by a ^{15}N pulse at point e and that magnetization evolves and is labeled for a time 2Tn until it is antiphase with respect to the $^{13}C'$ of the preceding residue, and is stored as 2NzC′z (point f). At point g, the 90° pulse applied on $^{13}C'$ creates the sum of two $^{13}C'$ coherences, one antiphase with respect to ^{15}N and the other antiphase with respect to $^{13}C^{\alpha}$. Until this point, the experiment is an interleaved combination of HNCO and HACACO. If the C′ chemical shift were to be sampled during t_2 as indicated in Figure 1E, the correlation of the NH(i) and ^{15}N(i) to $^{13}C^{\alpha}$(i–1) and $^{1}H^{\alpha}$(i–1) can in principle be obtained by realizing that corresponding pairs must appear on the same $^{13}C'$ plane (F2) in the 3D spectrum. For larger proteins, however, broader resonances combined with a poor $^{13}C'$ chemical shift dispersion (<20 ppm) cause many of such pairs to appear together on most C′ planes, making the connection of the pseudo-residue resonances impossible. To solve this problem, we use a pulse sequence that effectuates a bidirectional coherence transfer as indicated in Figure 1D.

During the (semi) constant-time evolution period 2Ta between points g and h, 180° pulses are applied on ^{15}N, $^{13}C'$ and $^{13}C^{\alpha}$ as indicated. A bidirectional coherence transfer occurs from 2NzC′x to 2CzC′x magnetization via the one-bond J couplings, and vice versa. Out- and-back HNCO and HACACO pathways ('out-and-back' peaks) are partially retained by specific delay choices (see below). The four coherence transfer pathways between periods g and h generate four cross peaks for every pseudo-residue in the 3D spectrum, arranged in a rectangular pattern. Thus, the ^{15}N(i) magnetization gives rise to an out-and-back peak at the amide region of the spectrum and a transfer peak at the $^{1}H^{\alpha}$(i–1) frequency, while the $^{13}C^{\alpha}$(i–1) magnetization gives an out-and-back peak at its H^{α} frequency and a transfer peak at the NH(i) chemical shift. In the periods h–n, magnetization is transferred back to the observable NH and $^{1}H^{\alpha}$ protons by the reverse of the process described above. Solvent suppression is achieved by purge pulses (after h) and a pulsed-field gradient.

The transfer can be calibrated by properly choosing the mixing periods (Ta*and*Tb). Figure 2 shows the efficiencies of the transfer and out-and-back pathways, which are influenced by the couplings $J_{NC'}$ and $J_{C^{\alpha}C'}$ and are given by:

out-and-backs:
$2NzC'x \longrightarrow 2NzC'x$
and $2CzC'x \longrightarrow 2CzC'x$:

$$\cos(\pi J_{NC'} 2Ta)\cos(\pi J_{C^{\alpha}C'} 2Tb) \quad (1)$$

transfers:
$2NzC'x \longrightarrow 2CzC'x$
and $2CzC'x \longrightarrow 2NzC'x$:

$$\sin(\pi J_{NC'} 2Ta)\sin(\pi J_{C^{\alpha}C'} 2Tb) \quad (2)$$

where 2Ta and 2Tb are the mixing times, and $J_{NC'}$ and $J_{C^{\alpha}C'}$ are the one-bond scalar couplings. As Figures 2A and B illustrate, if the mixing times are short, the transfer efficiency is low and only a fraction of 2NzC′x magnetization can be transferred to 2CzC′x and vice versa. For 2Ta equal to 13.2 ms and 2Tb equal to 5.2 ms, one obtains nearly equal amplitudes for transferred (0.48) and remaining coherences (0.49).

Changing the phases $\phi 3$ and $\phi 5$ by 180° causes the transfer peaks to flip their phase by 180°, while the out-and-back peaks retain their sign. Hence, by subtracting the spectra which are collected with different phases $\phi 3$ and $\phi 5$ one obtains the transfer peaks, while by adding them one obtains the out-and-back peaks.

Figure 3A shows the ^{1}H-[^{15}N,$^{13}C^{\alpha}$] plane, taken at a $^{13}C'$ resonance frequency 173.8 ppm of the 3D HNHCACO spectrum in which out-and-back peaks are positive and transfer peaks are negative. The positions of the four cross peaks per pseudo-residue along the F1

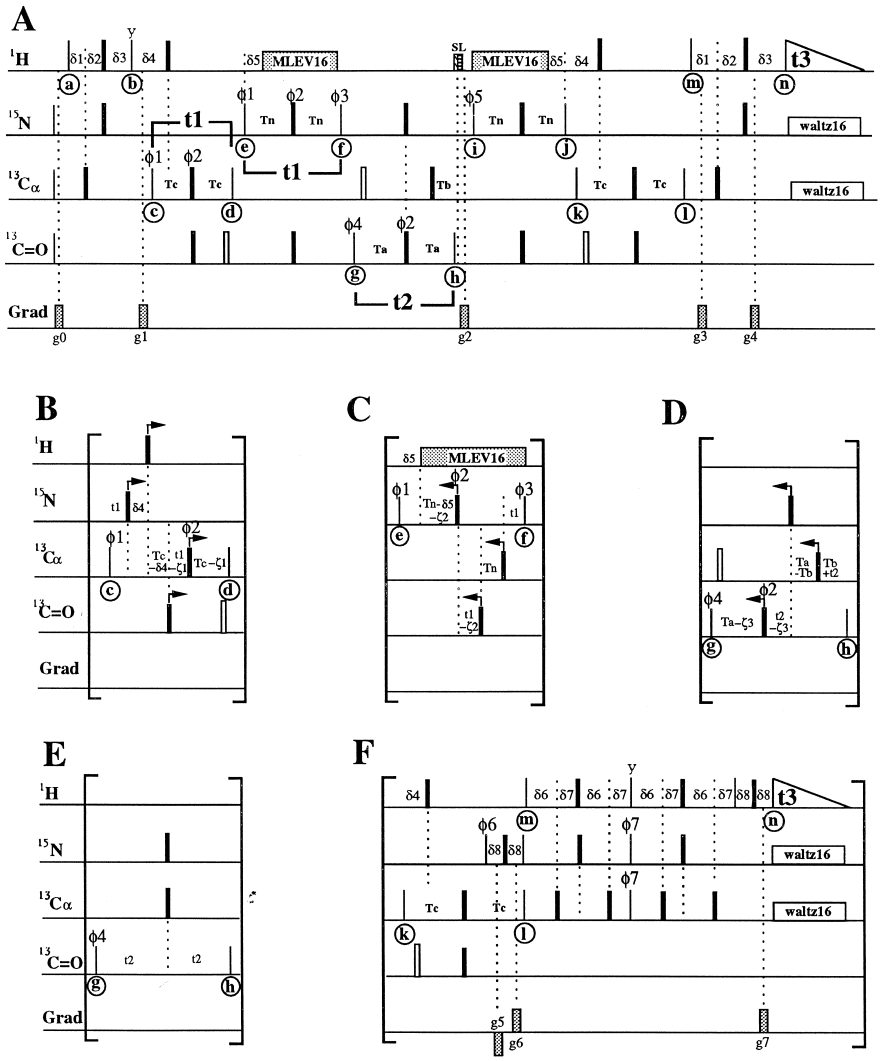

Figure 1. Pulse scheme for the 3D HNHCACO experiment. Narrow and wide bars denote pulses of 90° and 180° flip angles, respectively. Pulse phases are along the x-axis unless indicated otherwise. SL denotes 1 ms and 2 ms spin-lock pulses for solvent suppression (rf strength of 19.72 kHz) applied along the x- and y-axis. Rectangular pulse with pulse widths of 65 μs for 90° flip angles were used for both $^{13}C^{\alpha}$ and ^{13}CO, so that a null at the resonance frequency of the other carbon nucleus was obtained (500 MHz spectrometer); square pulses with 130 μs durations were used as carbon resonance inversion pulses. Field gradient pulses were sine-bell shaped of 1 ms duration, with typical strengths at the center of g0 = 24 G/cm, g1 = 24 G/cm, g2 = 18 G/cm, g3 = 30 G/cm, g4 = 30 G/cm. The period t_1 is the $^{13}C^{\alpha}$ and ^{15}N evolution time and the period t_2 is the ^{13}CO evolution time. In order to improve the digital resolution, semi-constant time labeling was applied for $^{13}C^{\alpha}$, ^{15}N and ^{13}CO as shown in schemes B, C and D, respectively. The Bloch–Siegert shifts were compensated with 180° pulses indicated with open boxes. The transfer delays were tuned accounting for the relaxation properties of the Binase (12.3 kDa), and were as follows: δ1 = 1.5 ms, δ2 = 1 ms, δ3 = 2.5 ms, δ4 = 1.5 ms, δ5 = 5.5 ms, Tc = 3.5 ms, Tn = 14 ms, Ta = 6.6 ms and Tb = 2.6 ms. The increments are: $\delta t_1 = 2 \times 180$ μs for $^{13}C^{\alpha}$ and 2×330 μs for ^{15}N, $\delta t_2 = 2 \times 330$ μs for ^{13}CO; ζ1 = 86 μs, ζ2 = 235 μs, ζ3 = 150 μs. The phase cycling is: ϕ1 = x,−x; ϕ2 = x,x,x,x,−x,−x,−x,−x; ϕ3 = −x, ϕ4 = x,x,−x,−x; ϕ5 =x; and receiver = +,−,−,+. States-TPPI quadrature detection was obtained by incrementation of ϕ1 and ϕ4 while inverting the receiver phase. Phases ϕ3 and ϕ5 can be alternated between +x and –x while storing the data in separate locations for out-and-back and transfer peak distinction (see text). The spectral widths for $^{13}C^{\alpha}$,^{15}N, ^{13}CO and ^{1}H are 2778 Hz (F1), 1515 Hz (F1), 1515 Hz (F2), 8333 Hz (F3). $36 \times 43 \times 1024$ complex points were collected with final semi-constant acquisition times of 13 ms (t_1,$^{13}C^{\alpha}$), 23.8 ms (t_1,^{15}N), 28.4 ms (t_2,^{13}CO) and 123 ms (t_3,^{1}H). The total measuring time of the 3D data set was 36 h using 32 scans per FID. Panel E shows a simplified experiment in which no transfer occurs. Panel F shows a dual frequency gradient coherence selection scheme. This scheme does not incur losses, except for relaxation in the additional refocussing periods. Gradients g5 and g6 are equal to 7 times and 3 times g7, respectively. Delays δ6, δ7 and δ8 are 2.175 ms, 0.425 ms and 1.0 ms, respectively. Phase ϕ6 equals −x. Phases ϕ7 are y and –y and are cycled together with inverting the sign of the gradient g7, while storing the data in separate locations. The spin-lock pulses 'SL' (see panel A) are not used in this solvent suppression scheme.

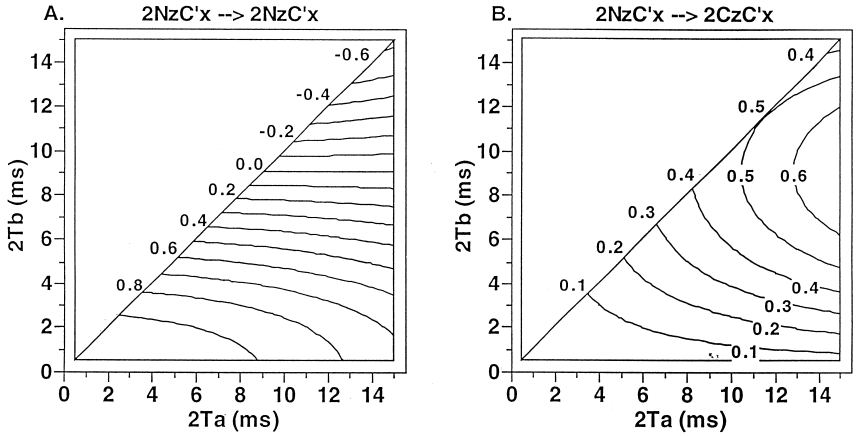

Figure 2. Calculations of the $2NzC'x \leftrightarrow C'y \leftrightarrow 2CzC'x$ transfer as a function of the heteronuclear ($J_{NC'}$, 16 Hz) coherence transfer time $2T_a$ and the homonuclear ($J_{C^\alpha C'}$, 55 Hz) coherence transfer time 2Tb, neglecting $^{13}C'$ transverse relaxation (Equations 1 and 2).

and F3 dimensions give the chemical shifts of NH(i), $^{15}N(i)$ and $^{1}H^{\alpha}(i–1)$, $^{13}C^{\alpha}(i–1)$, while the $^{13}C'(i–1)$ chemical shift of the four cross peaks is given by the frequency of the plane along the F2 dimension. The rectangular cross-peak arrangement is exploited to easily identify those peaks which belong to an individual pseudo-residue. Spectral overlap appears to be no problem for the 12.3 kDa protein Binase. The sensitivity of the experiment is excellent as is illustrated by a cross section (Figure 3B). All pseudo-residue identifications could be obtained for Binase with this single spectrum. The exceptions are correlations involving Pro, for which NH region signals are obviously missing, and Gly residues, for which all $C^{\alpha}H$ region signals and the cross peaks in the NH region are missing because of the tuning of the δ1 delays. These patterns can be used for residue-type identification. Other missing correlations are those for which the H^{α} signals are obliterated by the residual H_2O noise. Both NH region signals are nevertheless present, from which one can then tentatively conclude that the H^{α} frequency must coincide with that of the H_2O signal. Note that this situation differs from that of the Gly-containing pseudo-residues. The cross section in Figure 3B shows that the water band is relatively narrow due to the good performance of the purge pulses and gradient in the sequence (see Figure 1A). It was possible to improve the solvent suppression further by gradient selection with recovery (Palmer et al., 1991; Kay et al., 1992), performed simultaneously for the $^{13}C^{\alpha}$ and ^{15}N coherence pathways. Note that such gradient selection will not recover the $\sqrt{2}$ in sensitivity loss associated with quadrature detection in t_1, because that labeling needs to occur in the first half of the experiment in order to obtain the desired transfer patterns. We are thus left with a net loss in sensitivity because of relaxation during the multiple refocussing periods, and the modification was not further pursued. However, since the sequence for simultaneous gradient selection is in itself interesting we have included it in Figure 1F.

The basic sensitivity of the 3D HNHCACO should be compared with those in the experiments available that provide the same information. The 3D HCACOCANH (Löhr and Rüterjans, 1995) experiment using a dimensionality reduction strategy depends on small one-bond and two-bond scalar couplings ($^{1}J_{C^{\alpha}N}$,$^{2}J_{C^{\alpha}N}$) to transfer coherence, which would not be suitable for larger proteins. Therefore, we compare the sensitivity between 3D HNHCACO and 4D or 5D HACA(CO)NNH (Boucher et al., 1992), both of which take the effective pathways to transfer coherence. The coherence transfer periods used in that experiment are identical to those used in the new experiment proposed here. The number of rf pulses per pathway are roughly the same and optimal tuning of the delays to compensate for relaxation loss should also be the same in both experiments. Nevertheless, there are several differences between the experiments that give rise to sensitivity differences. There are four additional losses of sensitivity in the H^{α}-C^{α}-C'-N-HN pathway in our experiment as compared to HACA(CO)NNH. First, loss occurs in HNHCACO because of non-ideal timing of the $H^{\alpha} \rightarrow C^{\alpha}$ INEPT transfers where the transverse relaxation of the ^{1}H spins bound to $^{13}C^{\alpha}$ will proceed longer than necessary in a single-tuned INEPT transfer (loss of

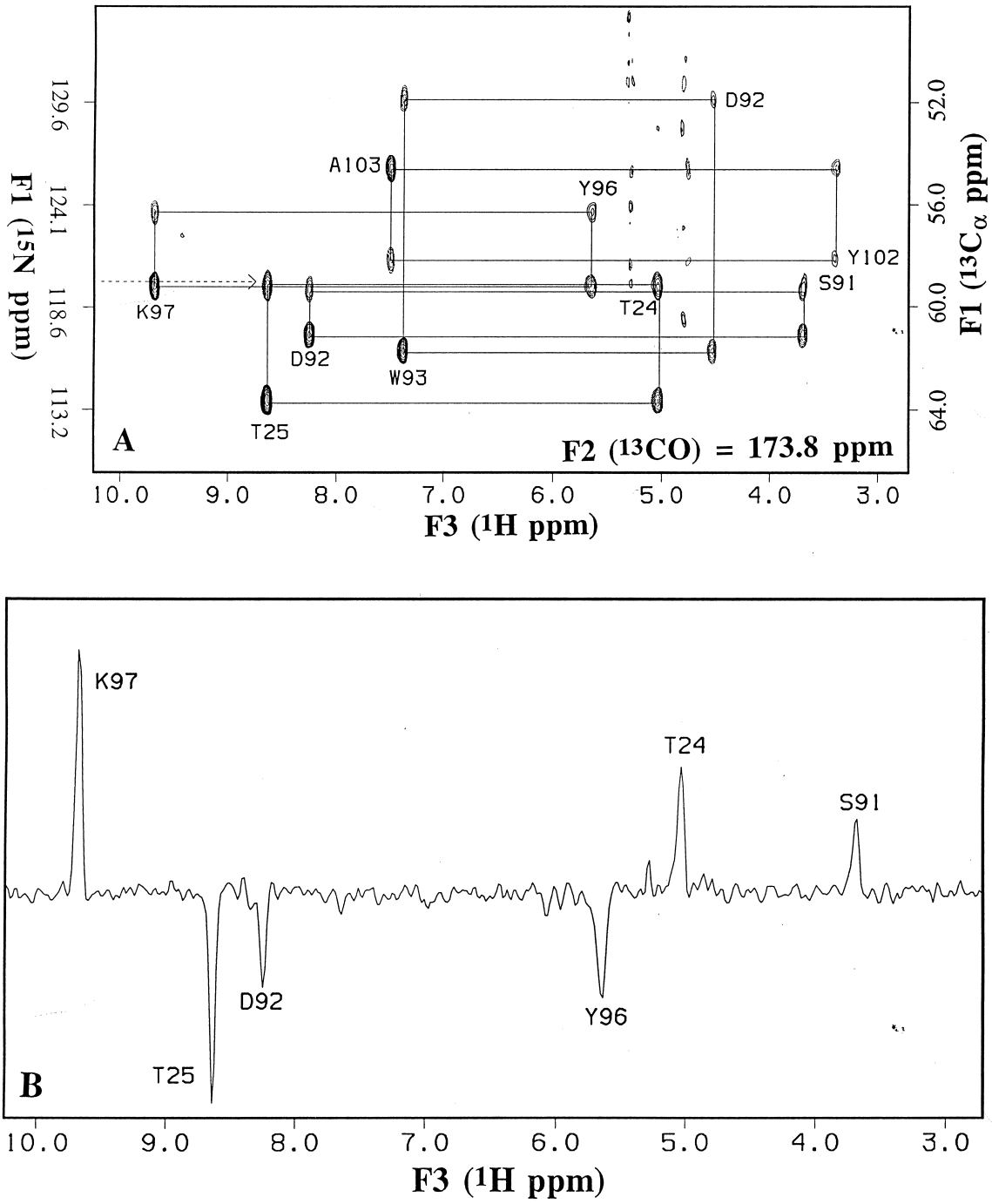

Figure 3. ^{1}H-[^{15}N, $^{13}C^{\alpha}$] slices of the 3D HNHCACO spectrum of 2.0 mM Binase (12.3 kDa), uniformly ^{13}C, ^{15}N-labeled and in 90:10 H_2O:D_2O, pH 7. Panel A shows the spectrum with positive out-and-back peaks and negative transfer peaks. Peak assignments are given at the positions of the out-and-back peaks. The negative contours are rendered with dashed lines. The four cross-peak components belonging to each pseudo-residue are connected by solid lines. Panel B shows a cross section through the data at the position of the dashed arrow in (A), demonstrating sensitivity and the level of solvent suppression. Assignments are given for both the positive out-and-back peaks as well as for the negative transfer peaks. The 3D HNHCACO spectrum was acquired in 36 h at 303 K on a Bruker AMX-500 spectrometer equipped with a 5 mm triple-resonance field gradient probe. Data processing was carried out with the program Felix 2.0 (a gift from Hare Inc.) and included a t_3-domain base line convolution with an averaging window of 10.8 ms.

approximately 5% for the 10 Hz ^{1}H NMR lines of Binase). Second, loss of 2CzC′z order occurs during the period e–f when ^{15}N evolution takes place. We estimate the characteristic relaxation time of such order as 500 ms from our measurement of 300 ms for this relaxation for a 20 kDa protein, leading to a loss of 6% over the 28 ms (initial) delay time 2Tn. Third, a 50% loss of signal occurs between g and h because of retention of both out-and-back and transfer pathways. Fourth, loss of 2NzHz order occurs during the period k–l when $^{13}C^{\alpha}$ refocussing takes place. The characteristic relaxation time of this order is estimated to be 120 ms from a measurement of 70 ms for a 20 kDa protein, leading to a loss of 6% over the 7 ms (initial) delay time 2Tc. In total, one computes for the H^{α}-C^{α}-C′-N-HN pathway in our experiment a sensitivity of 0.42 as compared to HACA(CO)NNH. As we use semi-constant time incrementation to obtain the necessary digital resolution (especially for the C^{α} evolution) additional losses occur, but those are likely offset by the loss in sensitivity in the semi-constant time acquisition of the H^{α} chemical shifts at the outset of the HACA(CO)NNH experiment. Overall, we argue that our experiment still competes in sensitivity with HACA(CO)NNH because of the following reasons. First, in order to obtain four or five frequencies, HACA(CO)NNH incurs losses of a factor $\sqrt{2}$ or a factor 2, respectively, because of rotational sense selection in the additional indirect dimensions – losses that cannot be (totally) recovered by gradient coherence selection. Second, sensitivity improvement in 3D HNHCACO comes upon data analysis from the expectation of finding the signals in a unique geometric arrangement (Simorre et al., 1994). A rectangular pattern of noise-level signals occurring on the same C′ plane is likely to be recognized as a real correlation, representing a sensitivity gain that is difficult to quantify. In total, we have that the sensitivities of the 3D HNHCACO experiment and the 4D/5D HACA(CO)NNH experiment should be roughly equal. Of course, the real virtue of the 3D HNHCACO experiment is that it resolves all five backbone frequencies (H^{α}(i–1), C^{α}(i–1), C'(i–1), NH(i), N(i)), at high resolution in only three dimensions. The 5D experiment capable of identifying that many frequencies in a single experiment has much lower digital resolution per dimension.

Acknowledgements

We thank Dr. M.W.F. Fischer and Dr. A. Majumdar for comments and discussions. This work was supported by Grant MCB 9513355 from the National Science Foundation and GM 52421 of the National Institutes of Health.

References

Bax, A. and Ikura, M. (1991) *J. Biomol. NMR*, **1**, 99–104.
Bax, A. and Pochapsky, S. (1992) *J. Magn. Reson.*, **99**, 636–646.
Boelens, R., Burgering, M., Fogh, R.H. and Kaptein, R. (1994) *J. Biomol. NMR*, **4**, 201–213.
Boucher, W., Laue, E.D., Campbell-Burk, S.L. and Domaille, P.J. (1992) *J. Biomol. NMR*, **2**, 631–637.
Brutscher, B., Cordier, F., Simorre, J.-P., Caffrey, M. and Marion, D. (1995) *J. Biomol. NMR*, **5**, 202–206.
Clore, G.M., Kay, L.E., Bax, A. and Gronenborn, A.M. (1991) *Biochemistry*, **30**, 12–18.
Clore, G.M. and Gronenborn, A.M. (1993) *NMR of Proteins*, CRC Press, Boca Raton, FL.
Clubb, R.T. and Wagner, G. (1992) *J. Biomol. NMR*, **2**, 389–394.
Farmer II, B.T. and Müller, L. (1991) *J. Magn. Reson.*, **93**, 635–641.
Farmer II, B.T., Venters, R.A., Spicer, L.D., Wittekind, M.G. and Müller, L. (1992) *J. Biomol. NMR*, **2**, 195–202.
Farmer II, B.T. and Müller, L. (1994) *J. Biomol. NMR*, **4**, 673–687.
Fesik, S.W. and Zuiderweg, E.R.P. (1988) *J. Magn. Reson.*, **78**, 588–593.
Grzesiek, S. and Bax, A. (1992) *J. Magn. Reson.*, **96**, 432–440.
Grzesiek, S. and Bax, A. (1993) *J. Biomol. NMR*, **3**, 185–204.
Ikura, M., Bax, A., Clore, G.M. and Gronenborn, A.M. (1990a) *J. Am. Chem. Soc.*, **112**, 9020–9022.
Ikura, M., Kay, L.E. and Bax, A. (1990b) *Biochemistry*, **29**, 4659–4667.
Jahnke, W. and Kessler, H. (1994) *J. Biomol. NMR*, **4**, 735–740.
Kay, L.E., Ikura, M., Tschudin, R. and Bax, A. (1990) *J. Magn. Reson.*, **89**, 496–514.
Kay, L.E., Keifer, P. and Saarinen, T. (1992) *J. Am. Chem. Soc.*, **114**, 10663–10665.
Löhr, F. and Rüterjans, H. (1995) *J. Biomol. NMR*, **6**, 189–197.
Mariani, M., Tessari, M., Boelens, R., Vis, H. and Kaptein, R. (1994) *J. Magn. Reson.*, **B104**, 294–297.
Montelione, G.T. and Wagner, G. (1990) *J. Magn. Reson.*, **87**, 183–188.
Palmer III, A.G., Cavanagh, J., Wright, P.E. and Rance, M. (1991) *J. Magn. Reson.*, **93**, 151–170.
Pascal, S.M., Muhandiram, D.R., Yamazaki, T., Forman-Kay, J.D. and Kay, L.E. (1994) *J. Magn. Reson.*, **B103**, 197–201.
Sattler, M., Maurer, M., Schleucher, J. and Griesinger, C. (1995) *J. Biomol. NMR*, **5**, 97–102.
Simorre, J.-P., Brutscher, B., Caffrey, M.S. and Marion, D. (1994) *J. Biomol. NMR*, **4**, 126–132.
Sørensen, O.W. (1990) *J. Magn. Reson.*, **89**, 210–216.
Szyperski, T., Wider, G., Bushweller, J.H. and Wüthrich, K. (1993) *J. Am. Chem. Soc.*, **115**, 9307–9308.
Wagner, G. (1993) *J. Biomol. NMR*, **3**, 375–385.
Zuiderweg, E.R.P., Petros, A.M., Fesik, S.W. and Olejniczak, E.T. (1991) *J. Am. Chem. Soc.*, **113**, 370–371.